Int J Thermophys (2008) 29:969–983
DOI 10.1007/s10765-007-0348-y

Large- and Small-Aperture Fixed-Point Cells of Cu, Pt–C, and Re–C

Klaus Anhalt · Yunfen Wang · Yoshiro Yamada · Jürgen Hartmann

Published online: 6 February 2008

Abstract Extending the application of metal (carbide)–carbon eutectic fixed-point cells to radiometry, e.g., for measurements in irradiance mode, requires fixed-point cells with large apertures. In order to make large-aperture cells more readily usable in furnace systems with smaller furnace tubes commonly used for small-aperture fixed-point cells, a novel cell design was developed. For each of Cu, Pt–C, and Re–C fixed points, two types of fixed-point cells were manufactured, the small- and large-aperture cell. For Pt–C and Re–C, the large-aperture cells were filled with a hyper-eutectic metal–carbon mixture; for the small cells, a hypo-eutectic mixture was used for filling. For each material, the small and large cells were compared with respect to radiometric differences. Whereas plateau shape and melting temperature are in good agreement for the small- and large-aperture Cu cells, a larger difference was observed between small- and large-aperture cells of Pt–C and Re–C, respectively. The origin of these observations, attributed to the temperature distribution inside the furnace, ingot contamination during manufacture, and non-uniform ingot formation for the larger cells, is discussed. The comparison of measurements by a radiation thermometer and filter radiometer of the Re–C and Pt–C large-aperture cells showed large differences that could be explained only by a strong radiance distribution across the cavity bottom. Further investigations are envisaged to clarify the cause.

K. Anhalt (✉) · J. Hartmann
AG 7.31 High Temperature Scale, Physikalisch-Technische Bundesanstalt,
Abbestr. 2-12, 10587 Berlin, Germany
e-mail: klaus.anhalt@ptb.de

Y. Wang · Y. Yamada
National Metrology Institute of Japan (NMIJ), AIST, AIST Tsukuba Central 3,
1-1-1 Umezono, Tsukuba, Ibaraki 305-8563, Japan

Keywords Filter radiometer · Fixed points · High temperatures · Metal–carbon eutectics · Radiation thermometry

1 Introduction

Metal (carbide)–carbon (M(C)–C) eutectic fixed-point cells have established themselves as highly-reproducible, stable, and useful tools in radiation thermometry with the advancements in cell manufacture and better understanding of furnace effects on their performance [1,2]. For those fixed points exceeding 2,200°C, there is special interest in the extension of their application to radiometry. Such applications, e.g., for direct measurements in the irradiance mode, require fixed-point cells with a large aperture, preferably exceeding 9 mm in diameter [3]. Such cells have been specially designed and tested for the VEGA blackbody (BB) furnaces [4]. With their wide inner furnace tube, these furnaces can hold M(C)–C eutectic fixed-point cells with the dimensions needed to maintain a high emissivity. However, such large-aperture fixed-point cells were found to be of poorer quality with wider melting ranges and non-ideal plateau shapes during the phase transformation when compared to the commonly-achievable realizations of small-aperture fixed-point cells used in radiation thermometry, typically of 3- or 4-mm aperture diameter [5]. Indicators for cell quality and plateau shape are a low melting range, i.e., the temperature range of the melting plateau with limited slope around the inflection point and the length of the plateau duration. Both reduce the uncertainty in determining the point of inflection of the melting plateau. In the case of the large-aperture fixed-point cells, a subsequent investigation to improve the temperature uniformity in the BB furnace showed that indirect radiative heating of the cells with additional thermal insulation surrounding the cell holder improves the plateau quality for a 3-mm-aperture cell [6]. A preliminary attempt to apply this method to a Re–C eutectic-point (2,474°C) large-aperture cell with an 8-mm aperture was reported in [3]. Here, the large-aperture cell retains the outer diameter of 24 mm so as to fit in the same holder as the small-aperture cell. However, the observed plateau was far from ideal.

In this work, we describe further investigations of the large-aperture cells for radiometry, again with the same diameter as the small-aperture cells. An attempt to improve the filling method is described, and the differences in performance between large- and small-aperture cells are studied systematically. Finally, measurements by radiation thermometers and filter radiometers, in the irradiance mode, are compared.

2 Cell Design and Fabrication

Two types of cells are employed in this investigation, the small-aperture (SA) cell and the large-aperture (LA) cell. Three fixed points are studied: Re–C eutectic, Pt–C eutectic (1,738°C), and Cu (1,084.62°C), and two SA and one LA cells are involved for each type. The material used came from the same supplier for each fixed-point type, but the production lot was different for the two SA cells (with the exception of Re), and the same for one SA cell and the LA cell. For all cells, one to three layers of 0.5-mm thick “C/C sheet” (manufactured by Toyo Tanso Co. Ltd, TCC-019) purified

Table 1 Specifications of the cells

Fixed-Point type	Nominal purity / Supplier	Metal Lot #	Cell ID	Cell design	Number of C/C layers	Metal Mass	Eutectic composition
Cu	99.999 %	D25N18	6ST-3	SA	3	21 g	–
	Alfa Aesar	J21Q086	PTB I	SA	2	27 g	–
		J21Q086	PTB LA I	LA	1	113 g	–
Pt-C	99.999 %	u09-032	H14	SA	2	55 g	0 % (hypo)
	Tanaka	u12-085	PTB I	SA	2	65 g	0 % (hypo)
	Kikinzoku	u12-085	PTB LA I	LA	2	71 g	2 % (hyper)
Re-C	99.999 %	05-KT-001	6SS-6	SA	2	64 g	1 % (hypo)
	ZKMTW	05-KT-001	PTB I	SA	2	57 g	1 % (hypo)
	China	05-KT-001	PTB LA I	LA	2	77 g	5 % (hyper)

carbon cloth material were placed inside the fixed-point cells between the crucible outer wall and the metal to optimize the temperature uniformity and to reduce the risk of cell breakage [3]. The list of cells with their specifications is given in Table 1. It is informative to explain the nomenclature that is conventionally used for the eutectic composition and reported in Table 1. For cell manufacture, high-purity graphite and metal powders, if mixed at the nominal eutectic metal–carbon composition, are found to form a non-uniform ingot, e.g., by the formation of holes [7], which remain even after melting of the metal due to the high viscosity of the eutectic material. These structural effects can be avoided by a metal–carbon mixture that is a few percent lower in carbon concentration than the original eutectic composition. Such a mixture is called *hypo*-eutectic, and additional graphite is taken from the crucible walls by the alloy to reach the eutectic composition during the first melts and freezes.

A metal–carbon mixture that is richer in carbon compared to the eutectic composition is termed *hyper*-eutectic. The *hyper*-eutectic metal can be sintered to form a uniform dense, but porous, structure that does not flow, even when molten, due to its high viscosity and due to the presence of graphite flake particles to which the metal adheres [8]. Due to its porosity, a *hyper*-eutectic ingot reduces the amount of metal necessary for cell filling. However, with less material in the same crucible volume, it was found that hyper-eutectic fixed-point cells have shorter melting and freezing plateaux, but no differences in the melting range and melting temperature were observed [8].

2.1 Small-Aperture (SA) Cells

The SA cell design is displayed in Fig. 1. The outer diameter is 24 mm, and the length is 45 mm. The crucible has a cavity with an aperture diameter of 3 mm, and a length of 33 mm, with a conical bottom having an apex angle of 120°. The wall thickness of the cavity is 2 mm. The emissivity of the cavity was calculated to be 0.9997. The space between the crucible inner wall and the cavity outer wall, which is filled with the C/C sheets and the ingot, is 4.5 mm. The number of C/C layers used inside the cell

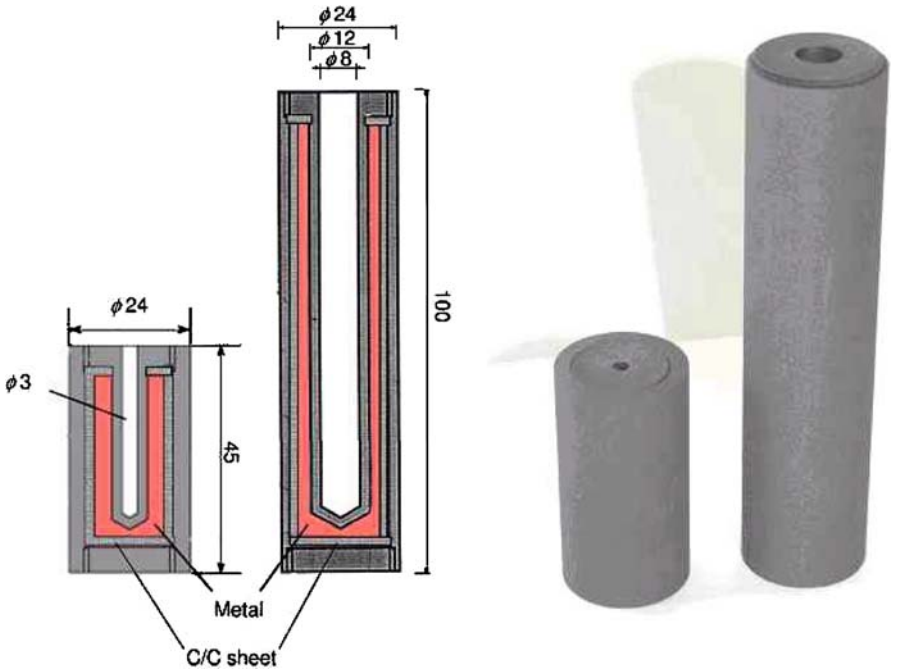

Fig. 1 Cell design used for Cu, Pt–C, and Re–C fixed-point cells, dimensions in mm

is determined by the space available. For the SA cells, two layers of C/C sheet leave a 3.5 mm channel for the eutectic ingot.

The filling procedure for the fixed-point cells followed the established routine at the National Metrology Institute of Japan (NMIJ) [9], using a vertical version of the common Nagano M as the furnace (Nagano VR20-A10) that is exclusively used to fill fixed-point cells.

2.2 Large-Aperture (LA) Cells

The LA cell design presented in Fig. 1 is the same as the cell in [3]. The crucible has a 24 mm outer diameter and a length of 100 mm. The cavity has a diameter of 8 mm and a length of 89 mm. The shape was designed to be similar to the cavity of the SA cell in order to achieve the same effective emissivity. The cavity wall has a thickness of 2 mm. The required large cavity aperture in conjunction with the crucible's outer diameter of 24 mm restricts the outer graphite walls of the crucible to a thickness of 2 mm. The thickness of the metal ingot plus the thickness of the C/C sheet around the cavity is 4 mm, which is smaller than the space available inside the SA cell, and for this reason, only one layer of C/C sheet was used for the LA cell.

The filling of the cell in [3] exposed some potential problems for the LA cell. The Re and Pt metals have densities of 21,020 $\mathrm{kg}\cdot\ \mathrm{m}^{-3}$ and 21,090 $\mathrm{kg}\cdot\mathrm{m}^{-3}$, respectively, values that are 2.7 times that of iron. If we continue to increase the aperture of the cells,

and therefore increase the dimensions of the cells, the high density of the metals will pose some problems. Firstly, the C/C sheet, will yield to the weight and compress as the metal height becomes higher during filling in a vertical furnace, and will no longer be able to buffer the stress arising from repeated melting and freezing. Secondly, the total mass of the cell, already exceeding 200 g [3] with the current-design LA cell, may become too heavy to be supported by the spring mechanism of the BB furnace heater (to be described below). The amount of metal is also directly reflected in the cost of the cell.

Therefore, in the current investigation, we attempted a new filling method to achieve a *hyper*-eutectic porous structure ingot with LA cells. In the LA crucible for the sintered metal ingot, ideal free shrinking of the ingot in all directions can be impeded by the long cavity dimension and by adhesion of the metal to the graphite cavity wall. As a result, the thin cylindrical ingot can tear, leaving parts of the cavity uncovered by the fixed-point material. Therefore, a special filling scheme was developed. To ensure uniform ingot formation, the filling was performed in sequential steps. In each step, the cells were filled with a *hyper*-eutectic metal–carbon powder mixture up to 20 mm in height and then sintered at a temperature 50–100 K below the material's eutectic melting temperature. The melting temperature was exceeded only after the cell was completely filled. Even after this step, the cavity and ingot can still be removed from the cell for visual inspection of the ingot due to the C/C sheets in the cell design. Ideally, the resulting ingot should be connected along the cavity wall and the step-wise filling procedure should not be visible in the resulting ingot. However, a non-uniform ingot was observed, which indicates that further improvement of the filling technique is required.

For Pt–C, parts of the sintered metal–carbon formed a metallic alloy during the final melting step, and this left two channels, each 2–3 mm wide, along the cavity wall uncovered. For Re–C, the number of filling steps was increased in order to form a sintered structure with each step, thus reducing the volume to be filled and making the structure more stable. Small gaps approximately 1–2 mm in width between each sintered filling structure resulted, but were filled in a final filling step.

The filling of the Cu LA cell was done in the same way as the SA cell.

3 Measurement Setup

3.1 Radiation Thermometer and Filter Radiometer

3.1.1 Radiation Thermometer

After preparation of the cells at NMIJ, the measurements were conducted at NMIJ and then at the Physikalisch-Technische Bundesanstalt (PTB). Two LP3 radiation thermometers [10] were used: LP3 80-40 for the measurements at NMIJ and LP3 80-05 at PTB. Both radiation thermometers use narrow-bandwidth interference filters with a central wavelength near 650 nm and have a target diameter of approximately 0.9 mm diameter at a measurement distance of 700 mm. The radiation thermometers were used for comparison purposes only, so the given temperatures are only radiance

temperatures and no statement about the absolute value of the fixed-point temperatures is made.

3.1.2 Filter Radiometers

The optical geometry for an irradiance measurement is defined by two precision apertures and the distance between them. One of the apertures is an integral part of the filter radiometer, which consists of an interference filter and a photodiode in a thermally stabilized housing. This aperture had a diameter of approximately 5 mm. A 3 mm precision aperture was used to define the radiating area of the blackbody.

Three filter radiometers were involved in the investigation, with center wavelengths of 476, 676, and 800 nm. These filter radiometers were characterized with respect to spectral irradiance responsivity traceable to the cryogenic radiometer RTCR of PTB [11]. The details of the filter radiometers and their setup principle are available in [5,12]. The 476-nm filter radiometer and the 3-mm precision aperture were hand-carried to NMIJ, where an optical stage was constructed to facilitate the alignment of furnace, furnace aperture, and filter radiometer.

3.2 Furnaces

For the investigations, four different furnaces were employed: two VEGA BB furnaces (BB3500YY and BB3200pg) and two Nagano furnaces (M and S). In the VEGA BB3500YY high-temperature furnace, a 355-mm long stack of pyrolytic graphite rings, with an inner diameter of 47 mm, is supported by a spring mechanism that becomes compressed with thermal expansion of the stack, and is directly electrically heated. In the central part of the furnace, a 150-mm-long carbon-fiber-reinforced carbon composite (C/C) holder with an inner diameter of 25 mm, wrapped outside with graphite cloth material for thermal insulation, holds the fixed-point cell. The specific electrical resistance varies for a set of pyrolytic graphite rings and the value differs for each ring. As a result, the rings will heat differently for the same nominal electrical current. This effect can be measured and is used to design the temperature uniformity inside the furnace by placing the rings accordingly. The furnace was optimized for temperature gradients following the technique presented in [6]. The HTBB3200pg, a smaller version of the BB3500YY furnace with a pyrolytic-ring inner diameter of 37 mm and a stack length of 290 mm, was used with a graphite holder of 105-mm length and 25-mm inner diameter. These furnaces were used mainly for LA cell measurements.

Details concerning the larger Nagano M furnace (Model VR10-A23), with a working temperature of up to 2,500°C, and the Nagano S furnace (Model VR10-A20), which is limited to 2,000°C, can be found in [13]. The performances of the two furnaces are considered effectively identical below 2,000°C. They were used solely for SA cells.

The BB3500YY and Nagano M and S furnaces were employed in the measurements at NMIJ, while the BB3200pg was used at PTB.

4 Plateau Observation

The fixed-point cells were evaluated by (a) comparing the two SA cells, (b) comparing the SA and LA cells, and (c) comparing measurements of the LA cells by a radiation thermometer and a filter radiometer in the irradiance mode. The presentation of the measurements focuses on a qualitative analysis of the plateau shapes during melting for Pt–C and Re–C and during freezing for Cu.

4.1 Cell Comparison with a Radiation Thermometer

4.1.1 Comparison of SA Cells

To verify the quality of the SA cells, and thereby the quality of the material lot and handling procedures used, a comparison of the SA cell pairs was first made with a radiation thermometer. For Cu and Pt–C, the Nagano M and S furnaces were used, while for Re–C, the VEGA BB3500YY was used together with the Nagano M furnace.

4.1.1.1 Cu The Cu PTB I cell was installed in the Nagano M furnace and the Cu 6ST-3 fixed-point cell in the Nagano S furnace. The furnace temperature was varied in temperature steps of ±20, ±10, and ±20 K, where the temperature values are the constant furnace set-point offsets relative to the fixed-point temperature for the melt and the freeze. Figure 2 shows a typical melt and freeze curve initiated by a ±20 K furnace-temperature step. The repeatability of the freezing temperature, evaluated by the standard deviation of the highest temperature during the freeze, was better than 10 mK for both cells and the temperature difference between the two cells was within 20 mK.

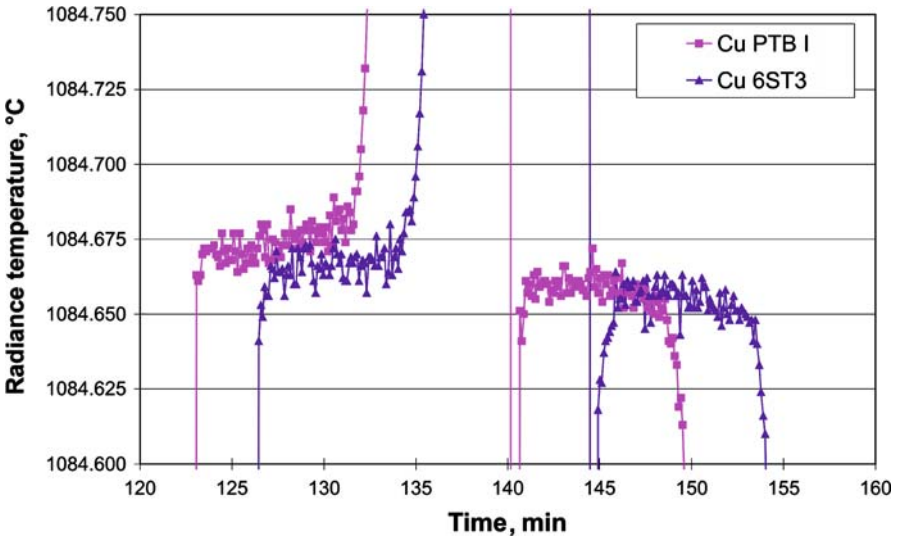

Fig. 2 Typical melting/freezing plateaux for SA copper fixed points

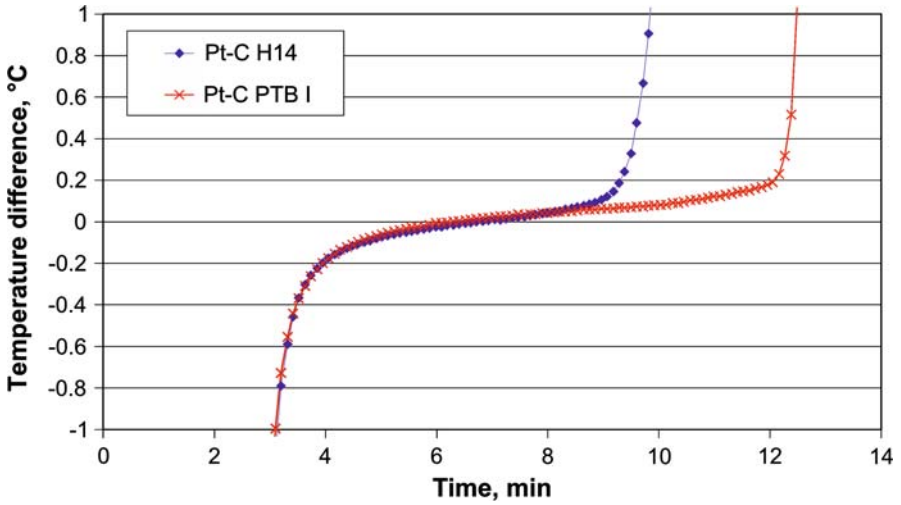

Fig. 3 Typical melting plateaux for SA Pt–C fixed-point cells

4.1.1.2 Pt–C The Pt–C PTB I cell was installed in the Nagano M furnace and the Pt–C H14 cell in the Nagano S furnace. Melting and freezing cycles were initiated with temperature steps of ±30, ±20, and ±10 K. Figure 3 shows a typical melting plateau for a temperature step of ±20 K. The repeatability of the melting temperature, evaluated at the inflection point, for three melts was 22 mK for Pt–C PTB I and 11 mK for Pt–C H14; the melting temperatures differed by less than 30 mK. For both cells, the melting range, evaluated as the melting-plateau slope at the inflection point times the plateau duration, is below 250 mK and the melt finishes with a sharp rise in temperature, which indicates both good cell quality and furnace temperature uniformity. Of the two cells, Pt–C PTB I contains a 20% larger metal ingot, which is directly reflected in the longer melting plateau for this cell.

4.1.1.3 Re–C The Re–C PTB I cell was installed in the BB3500YY furnace and compared to the Re–C 6SS-6 cell in the Nagano M furnace. Melt and freeze cycles were initiated with temperature steps of ±30 and ±20 K. Figure 4 shows a typical melting plateau for a temperature step of ±20 K. The repeatability was 16 mK for Re–C PTB I cell and 12 mK for Re–C 6SS-6. For both cells, the melting range is below 200 mK and the melt starts and finishes sharply.

4.1.2 Comparison of SA Versus LA cells

Next, the SA and LA cells were compared with a radiation thermometer. Only cells with the same material lot were chosen so that material purity would not be a factor in any observed differences. For this comparison, the LA cells were placed in the VEGA BB3500YY furnace while the Nagano M furnace was used for the SA cells.

4.1.2.1 Cu Figure 5 shows typical plateaux for a temperature step of ±20 K. Similar melting and freezing behavior for both fixed-point-cell designs were observed. For the large-aperture cell, the temperature was stable within 20 mK during the freeze over a

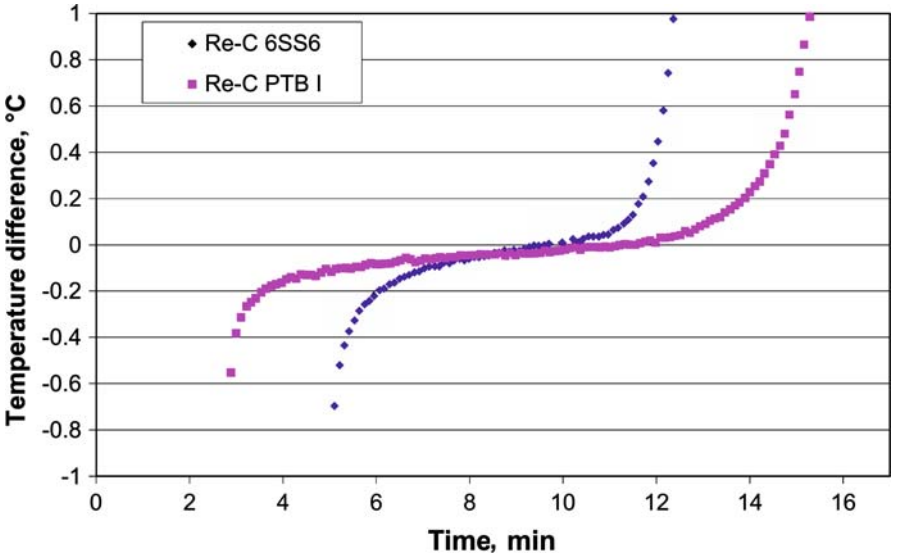

Fig. 4 Typical melting plateaux for SA Re–C fixed-point cells

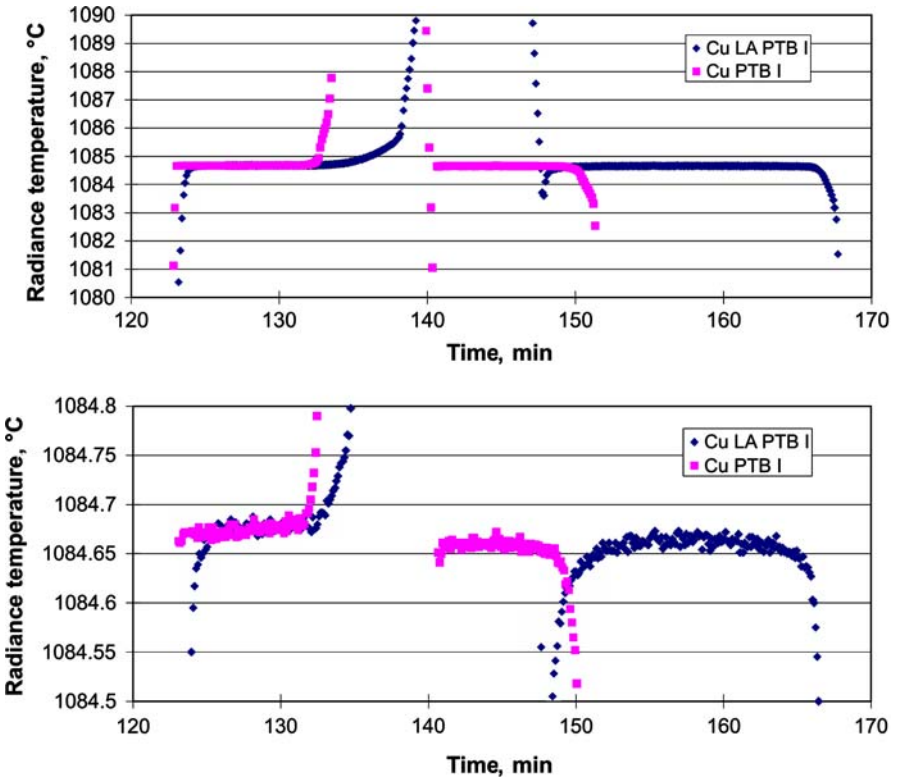

Fig. 5 Comparison of SA and LA Cu fixed-point cells

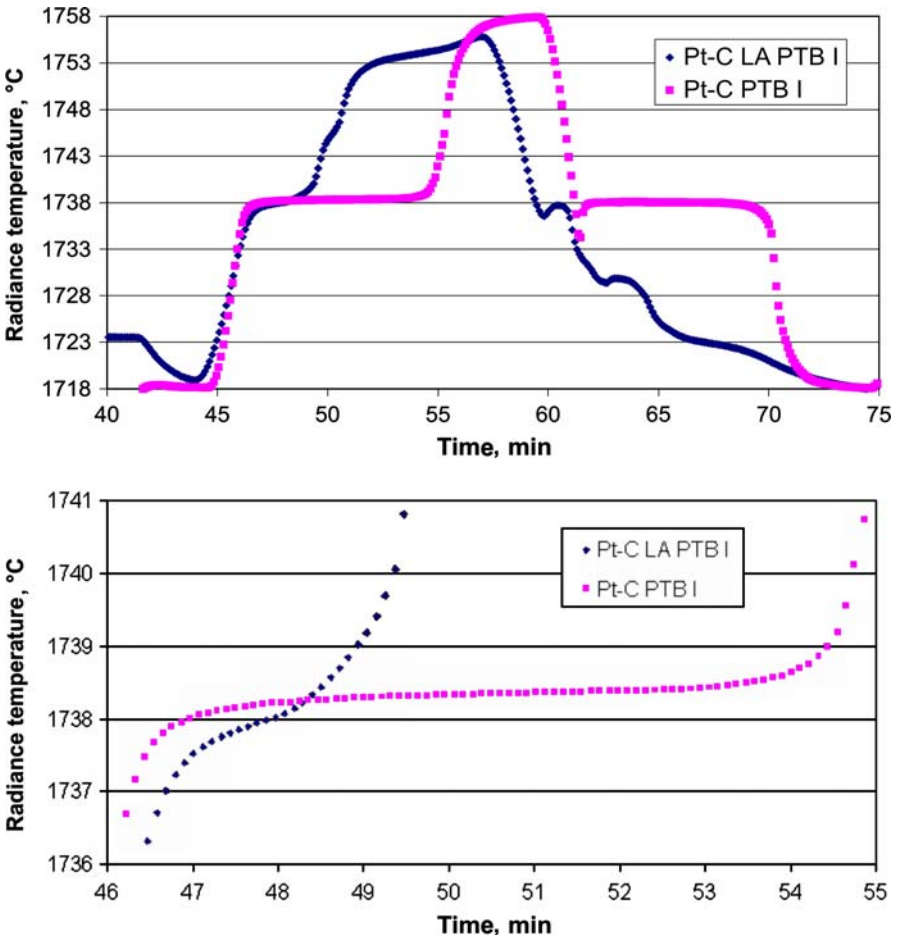

Fig. 6 Comparison of SA and LA Pt–C fixed-point cells

period of more than 15 min. Repeatability of the freezing temperature of 5 mK was observed for the large-aperture cell. Both cells show agreement to better than 20 mK for the freeze. Although the mass of the copper ingots differ significantly, the plateau duration is similar for both cells.

4.1.2.2 Pt–C For Pt–C, the observed melt and freezes are given in Fig. 6 for step changes of the furnace temperature of ±20 K. For the LA cell, the melting and freezing plateaux show different principal features: (a) the duration is significantly shorter, (b) the melting range is larger than 1 K, (c) the temperature rise at the end of the melt is not sharp, and (d) the temperature rise/fall after the melt and freeze do not start steadily with a continuous slope—instead, several structural features are seen. The repeatability of the melting temperature for the LA cell was found to be 74 mK. The LA cell showed a 450 mK lower temperature than the SA cell.

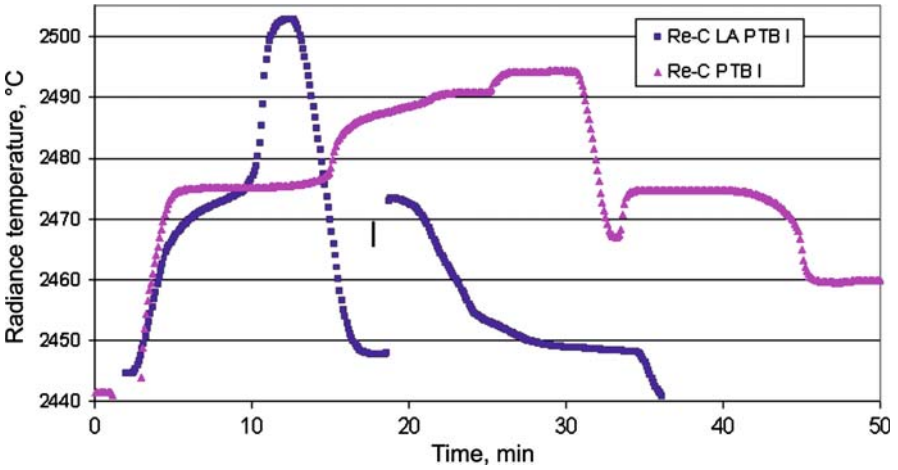

Fig. 7 Comparison of SA and LA Re–C fixed-point cells

4.1.2.3 Re–C For Re–C, a typical melting and freezing curve is depicted in Fig. 7 with a temperature step of ±30 K for the LA cell and −30 K/+15 K/−15 K for the SA cell. In this case, the melt is not only shorter for the LA cell, but also several kelvin lower in temperature. Furthermore, the melting range is larger than 5 K. The repeatability of the Re–C LA cell was 94 mK.

4.2 Comparison of Radiation Thermometer Versus Filter Radiometer Measurements for LA Cells

For each material, the LA cells were compared with respect to radiometric differences in plateau shape when measured in the radiance (i.e., with a radiation thermometer) or irradiance (i.e., with a filter radiometer) mode. For Pt–C and Re–C, the cells were measured at NMIJ using a filter radiometer with a central wavelength of 476 nm. Here, the distance between the two apertures was approximately 1,010 mm. Cu and Pt–C cells were measured at PTB using filter radiometers at 676 nm and 800 nm and a distance of around 1,115 mm between the two apertures. The cells were first measured with the filter radiometer, then the precision aperture in front of the furnace was removed and a set of measurements with the radiation thermometer followed. Typical melting/freezing plateaux that were initiated with step changes in the temperature furnace of ±20 K are plotted in Fig. 8.

While nearly identical freezing plateaux are observed for Cu, differences in the melting plateau for the other two LA cells are apparent. For Pt–C, the differences are pronounced at the end of the melt when the temperature rises, and for Re–C, the melting plateaux even show different slopes.

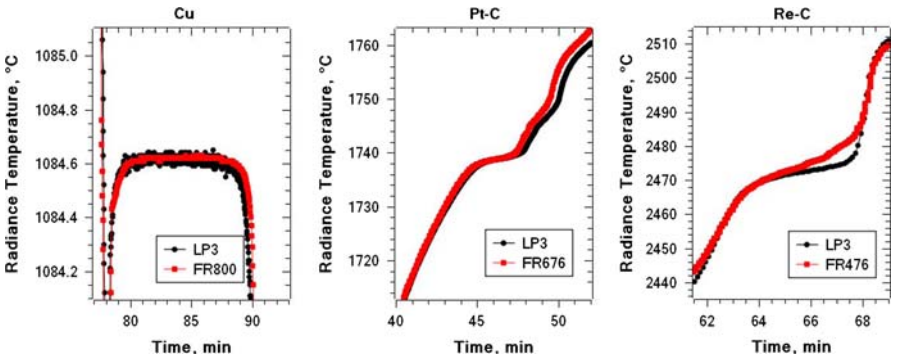

Fig. 8 Comparison between filter radiometer and radiation thermometer measurements for Cu LA I, Pt–C LA I, and Re–C LA I

5 Discussion

5.1 Comparison of SA Cells

No principal differences with respect to performance were observed between the two SA cells for Cu, Pt–C, and Re–C. Therefore, it can be concluded that the metals are of sufficient purity (for Re–C, the same batch was used) and that the routines for filling and handling were adequate in the case of the SA cells.

5.2 Comparison of SA and LA Cells

The Re–C and Pt–C LA cells exhibited lower temperatures and larger melting ranges. All three showed relatively shorter plateau durations. The differences in plateau temperature and melting range between LA and SA cells must be related to the ingot formation, impurity intake during filling, and insufficient temperature homogeneity of the cavity and the furnace used for the LA cell.

In contrast to the Cu-point cells, which have more uniform formation of the ingot and therefore a more homogeneous temperature distribution across the cell during the freeze, agreement of the two cells of Pt–C and Re–C is poor. This may be explained by the imperfect formation of the ingot around the cavity, as seen when inspecting the ingot during cell filling.

It is likely that the large difference for Re–C is caused by intake of impurities during the filling of the *hyper*-eutectic ingot LA cell. This statement is supported by an observation that, for the first melts and freezes, both melting and freezing temperatures decreased rapidly with increasing melting range, yet a visual inspection showed no signs of drastic changes in the physical shape of the sintered ingot.

In earlier studies, it has been shown that the cooling of the cavity wall that takes place due to radiative exchange with the colder environment outside the furnace increases drastically with temperature [14]. The effect is a non-uniform temperature drop across the cavity wall that leads to temperature inhomogeneity along its inner

surface. Furthermore, the effective emissivity of the radiator is affected by the temperature gradient in the furnace outside the cavity, and also inside along the cavity wall [15]. Based on the results of an analytical model, a temperature-drop difference of up to 400 mK and a radiance temperature difference of 250 mK can be expected for Re–C between fixed-point cells with a 3-mm and an 8-mm aperture [14]. The temperature difference observed here for the Re–C LA and SA cells is an order of magnitude larger, even though the LA cavity is longer than the one treated in [14]. The temperature-drop effect and the effective-emissivity effect cannot explain the observed difference. However, the model deals only with a uniform temperature distribution around the ingot, and therefore it would be of interest to model the transient melting curve in the presence of non-uniform ingot shapes, or non-uniform melting of the ingot due to temperature non-uniformity.

The plateau durations for the LA cells are only slightly longer (Cu) or shorter (Re–C, Pt–C) than the SA cells, even though they contain ingots of greater mass. However, one should realize that it is not the mass that is directly related to the plateau duration, but the ingot thickness (and the temperature difference across it). The LA cells have roughly the same thickness (Cu, Re–C) or 30% thinner (Pt–C) ingots as compared to the SA cells, and if one considers the porosity of the *hyper*-eutectic ingots (Re–C, Pt–C), the effective thickness is even thinner, and this explains the relatively short plateau durations.

5.3 Comparison of Radiation Thermometer Versus Filter Radiometer Measurements

At first glance, the observed differences are surprising. However, the radiance and irradiance modes differ in these experiments in the area that is seen by the instrument: when focused at the front aperture of the fixed-point cell, the LP3 has a measurement spot size about 2.5 mm in diameter at the bottom of the cavity; the filter radiometer, in conjunction with a distance between apertures of approximately 1 m, detects irradiance from an area 5.5 mm in diameter at the bottom of the cavity. From the discrepancies here, a non-ideal radiance distribution of the cavity bottom during the phase transition has to be concluded for the LA cells of Pt–C and Re–C. A similar inhomogeneous radiation field has been observed recently for cells of wider design. The cause for such large radiance distributions will be addressed in future investigations.

5.4 Future Work

A follow-up to the current investigation is envisaged, concentrated along the following topics:

5.4.1 Further Improvements to Furnace Uniformity

A new BB3500MP furnace with a 59-mm inner heater ring diameter is currently installed at PTB. The wide inner diameter gives more space for radiative heat exchange between the furnace tube and the fixed points and promises to improve the temperature gradient along the cells, and thus the effective emissivity of the cells.

5.4.2 Advanced LA Cell Design

Keeping the same calculated emissivity, a 6–7 mm aperture diameter cell requires a shorter total length, which reduces the temperature gradient across the cell in existing furnaces. Secondly, with a smaller cavity diameter for the same outer-cell diameter, the ingot thickness along the cavity can increase, which should help to improve the uniform ingot formation. Lastly, concentrating on special cells for BB furnaces allows also a wider outer-cell diameter with the described benefits for ingot formation.

5.4.3 Better Understanding of the Effect on the Plateau Shape of Hyper- and Hypo-eutectic Ingots in a Non-ideal Temperature Profile

With the proposed improvements to the LA cell design, the graphite wall thickness can also be increased, yielding more robust cells. Such cells can be filled with both *hyper*- and *hypo*-eutectic ingots, without the danger of breaking or cracking, and an optimized *hyper*-eutectic ingot can then be compared to *hypo*-eutectic fixed-point cells.

6 Conclusion

We demonstrated that an 8-mm diameter cavity design could be implemented in a 25-mm diameter tube furnace and measured with a filter radiometer using a 3-mm diameter precision aperture in front of the furnace.

The metal–carbon eutectic LA cells showed relatively poor plateaux as compared to SA cells. Possible causes are: (a) the non-ideal cell design of the LA cells, which leaves only a narrow channel around the cavity for the metal ingot, resulting in imperfect cell manufacture, with a non-continuous metal ingot, for Pt–C and Re–C, (b) contamination during ingot handling in the *hyper*-eutectic filling stage, and (c) insufficient temperature uniformity of the furnace, which has a larger effect on the longer LA cells. The causes for the observations made here should be further investigated, and improvements in furnace-temperature homogeneity, cell design, and cell fabrication technique are necessary.

When this is accomplished, a direct irradiance-mode measurement to determine the thermodynamic temperature of the M(C)–C eutectic fixed points becomes possible.

Acknowledgments The authors are indebted to Y. Bitou and Dr. S. Telada from the length section of NMIJ for their support in establishing a reliable distance measurement, and to K. Yamazawa from the thermometry section and Y. Ichino of the radiometry section of NMIJ for help with electrical measurements and calibrations. **Disclaimer** Certain commercial equipment, instruments, or materials are identified in this paper in order to adequately describe the experimental procedure. Such identification does not imply recommendation or endorsement by the authors, nor does it imply that the materials or equipment identified are the only or best available for the purpose.

References

1. Y. Yamada, MAPAN-J. Metrol. Soc. India **20**, 183 (2005)
2. E. Woolliams, G. Machin, D. Lowe, R. Winkler, Metrologia **43**, R11 (2006)
3. Y. Yamada, B. Khlevnoy, Y. Wang, T. Wang, K. Anhalt, Metrologia **43**, S140 (2006)

4. V. Sapritsky, S. Ogarev, B. Khlevnoy, in *Temperature: Its Measurement and Control in Science and Industry*, vol. 6, Part 1, ed. by J.F. Schooley (AIP, New York, 2002), pp. 377–382
5. J. Hartmann, K. Anhalt, M. Sakharov, B. Khlevnoy, A. Bourdakin, in *Proceedings of TEMPMEKO 2004, 9th International Symposium on Temperature and Thermal Measurements in Industry and Science*, ed. by D. Zvizdić, L.G. Bermanec, T. Veliki, T. Stašić (FSB/LPM, Zagreb, Croatia, 2004), pp. 189–194
6. B. Khlevnoy, M. Sakharov, S. Ogarev, V. Sapritsky, Y. Yamada, K. Anhalt, in *Proceedings of TEMPMEKO 2007*, Int. J. Thermophys., doi: 10.1007/s10765-007-0347-z
7. Y. Yamada, H. Sakate, F. Sakuma, A. Ono, in *Proceedings of TEMPMEKO '99, 7th International Symposium on Temperature and Thermal Measurements in Industry and Science*, ed. by J.F. Dubbeldam, M.J. de Groot (Edauw Johannissen bv, Delft, 1999), pp. 535–540
8. Y. Yamada, P. Bloembergen, in *Proceedings of TEMPMEKO 2004, 9th International Symposium on Temperature and Thermal Measurements in Industry and Science*, ed. by D. Zvizdić, L.G. Bermanec, T. Veliki, T. Stašić (FSB/LPM, Zagreb, Croatia, 2004), pp. 171–176
9. D. Lowe, Y. Yamada, Metrologia **43**, 135 (2006)
10. J. Fischer, G. Neuer, E. Schreiber, R. Thomas, in *Proceedings of TEMPMEKO 2001, 8 International Symposium on Temperature and Thermal Measurements in Industry and Science*, ed. by B. Fellmuth, J. Seidel, G. Scholz (VDE Verlag, Berlin, 2002), pp. 801–806
11. D.R. Taubert, R. Friedrich, J. Hartmann, J. Hollandt, Metrologia **40**, S35 (2003)
12. K. Anhalt, J. Hartmann, D. Lowe, G. Machin, M. Sadli, Y. Yamada, Metrologia **43**, S78 (2006)
13. Y. Yamada, N. Sasajima, H. Gomi, T. Sugai, in *Temperature: Its Measurement and Control in Science and Industry*, vol. 6, Part 1, ed. by J.F. Schooley (AIP, New York, 2002), pp. 985–990
14. P. Jimeno-Largo, Y. Yamada, P. Bloembergen, M.A. Villamanan, G. Machin, in *Proceedings of TEMPMEKO 2004, 9th International Symposium on Temperature and Thermal Measurements in Industry and Science*, ed. by D. Zvizdić, L.G. Bermanec, T. Veliki, T. Stašić (FSB/LPM, Zagreb, Croatia, 2004), pp. 335–340
15. P. Bloembergen, B. Khlevnoy, P. Jimeno-Largo, Y. Yamada, in *Proceedings of TEMPMEKO 2007*, Int. J. Thermophys., doi: 10.1007/s10765-007-0323-7